Title	Fluid lubrication model over sinusoidal roughness with streamline-based approach
Author(s)	Okazaki, Haruki; Takeuchi, Shintaro
Citation	Microfluidics and Nanofluidics. 2024, 28(30), p. 402
Version Type	AM
URL	https://hdl.handle.net/11094/95262
rights	© The Author(s), under exclusive licence to Springer-Verlag GmbH Germany, part of Springer Nature 2024
Note	

Accepted Manuscript
Microfluidics and Nanofluidics (2024)
https://doi.org/10.1007/s10404-024-02721-3

Fluid lubrication model over sinusoidal roughness with streamline-based approach

Haruki Okazaki[1] **and Shintaro Takeuchi**[1*]

[1] Department of Mechanical Engineering, Osaka University,
2-1 Yamada-oka, Suita, Osaka 565-0871 Japan

Abstract

A method is proposed to deterministically obtain steady lubrication pressure for the Stokes flow in a channel bounded by a flat wall and a surface with roughness represented by sinusoidal waves. A streamline sufficiently far away from the rough surface is used to formulate a streamline-based lubrication equation with the velocity on the streamline, and the velocities on the streamline is imposed as a boundary condition. In the solution of the lubrication equation, by virtually moving the streamline towards the flat wall, the pressure on the flat wall is obtained, and then the wall-normal variation of the pressure is recovered from the wall pressure by a lubrication model that considers higher order terms. The proposed method is applied to lubrication flows in channels with roughness represented by a single sinusoidal wave and a superposition of several sinusoidal waves. Through comparison with analytical solutions, the validity of the proposed method is established, and the applicable range of superposition of waves is explained that lowest-wavenumber component in surface profile is sufficiently isolated from higher-wavenumber components. Although the problem setting intrinsically prohibits the application of the conventional Reynolds lubrication equation, this study provides new understandings for the pressure obeying the Reynolds lubrication equation and the role of the higher-order terms.

keywords: Lubrication pressure, Wall-normal pressure distribution, Sinusoidal roughness, Deterministic treatment

*Corresponding author: shintaro.takeuchi@mech.eng.osaka-u.ac.jp, ORCID ID: 0000-0003-0091-4542

1 Introduction

When two facing surfaces move relatively to each other with a small gap, lubrication pressure develops in the region between the surfaces. For non-circular or non-spherical geometry, the lubrication pressure is often predicted by solving the Reynolds lubrication equation [1]. However, the equation is derived based on a number of assumptions for working fluid and wall geometry. One of the assumptions for the Reynolds lubrication equation is negligibly small gap width; aspect ratio α (i.e. the ratio of the gap distance to the longitudinal characteristic length) of the channel being $\alpha \ll 1$, which enables treatment of the pressure (in the Reynolds lubrication regime) to be independent of the distance from the wall surface. However, this assumption may not be satisfied for a surface with roughness.

Surface roughness and aspect ratio are not independent for predicting the lubrication pressure; Elrod [2] showed that the conditions for applying the Reynolds lubrication equation is related to the local aspect ratio (H/L') of the average clearance H to the roughness wavelength L' (see Fig. 1), and Bayada and Chambat [24] pointed out that lubrication with roughness is classified depending on the mean height of the channel and roughness period. Therefore, if the roughness is not negligible, the condition of the aspect ratio has to be reconsidered for deriving effective lubrication equation. Moreover, if the local aspect ratio is regarded as not small, the independence of the pressure on the wall-normal distance may no longer be valid, resulting in pressure variations in the normal direction to the nominal surface.

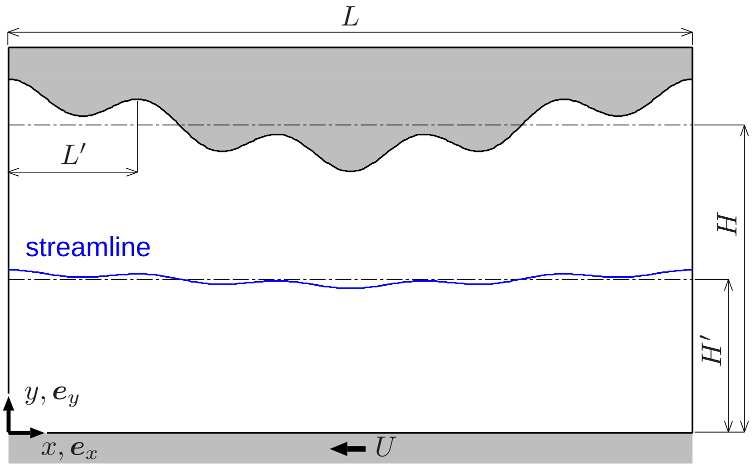

Figure 1: Schematic of a general case of lubrication in a region between a roughness wall and moving flat wall. In the present study, one streamline away from the wavy wall is selected to impose the boundary condition to calculate the pressure on the flat wall, and the pressure distributions in both wall-tangential and wall-normal directions are recovered by an original higher-order lubrication model.

There are mainly two ways for relating wall roughness to fluid lubrication in the previous studies: stochastic and deterministic approaches. Stochastic treatment assumes roughness superposed on the smooth nominal surface and extracts the statistical quantities of the geometry (e.g. nominal height and standard deviation), and these are reflected to the Reynolds lubrication equation as modified or additional term. Christensen [3] restricted the roughness to one dimension and developed a stochastic Reynolds lubrication equation based on an approach of average film thickness (i.e. arithmetic and harmonic averages for the longitudinal and transverse roughness), and later Mitsuya [4] improved the approach to use a mixed-average film thickness of arithmetically and harmonically averaged thickness to derive a mixed-average Reynolds lubrication equation. On the other hand, Patir and Cheng [5, 6] employed an average-flow approach that includes flow roughness modification factors to the Reynolds lubrication equation. In their study, the modification factors are obtained numerically, whereas Tripp [7] obtained the modification factor analytically for random surface profiles using the perturbation method. Later, Sahlin et al. [8] used the homogenisation technique to separate the effect of the local roughness scale from the global scale, and they obtained the factor for given roughness geometries. Almqvist et al. [25] proved that the flow factor method by Patir and Cheng coincides with the result of the homogenisation only when a certain symmetry exists in roughness profile. However, a common problem in the above methods is that, as the effect of roughness is only included as modification factors to the Reynolds lubrication equation, the pressure variation in the vertical direction of the nominal wall is not considered. Friction-reducing devices are not the only cases in which this problem manifests itself. In particle-laden flows, for example, careful numerical treatments are necessary to capture the complex pressure distributions in the interparticle region of relatively-moving particles even for a case of smooth surfaces [9, 10], and the complexity in the pressure distribution may increase with roughness. The effect of roughness also appears on the propulsion of microorganism swimming with a undulating surface motion above a rough surface [11]. Therefore, considering that local aspect ratio influences the lubrication, it is necessary to explore an advanced idea to calculate the distribution of the lubrication pressure in both longitudinal and transverse directions above the rough surface.

On the other hand, in deterministic approaches for roughness, direct or approximate treatment of the geometry gives a precise view of the problem [12]. However, mathematical representation of the roughness may become complex as randomness enhances, and therefore, it is not always easy to predict the flow field by this approach. Some types of machined surfaces can still be described deterministically. Roughness properties are characterised by machine processing as follows [13]: when the surface is repeatedly machined (e.g. peening) the surface tends to have a random roughness and the probability distribution becomes close to Gaussian, whereas, for one-time machining operations such as turning, the surface height follows non-Gaussian distribution. Besides machined surfaces, there may be artificially-formed roughness;

experimental study [14] showed that surface texturing may be effective in maintaining the load-bearing performance. Jeong and Son [15] placed semi-circular protuberances on microchannel walls, and they analytically studied that the viscous flow through the microchannel departs from the solution of the Reynolds lubrication equation under non-negligible gap width.

In both stochastic and deterministic ways, under situations where the Reynolds lubrication equation does not hold (i.e., non-negligible aspect ratio associated with roughness), the velocity and pressure profiles depart from those in a simple channel flow, and reconsideration from a fundamental viewpoint is needed.

In this paper, to study fundamental effect of roughness on lubrication pressure, roughness is expressed by superposition of sinusoidal waves and its effect on the flow field is treated deterministically. To establish a method for pressure reconstruction in the wall-normal direction in a channel with roughness, two-dimensional incompressible steady flow in the Stokes regime [16] is treated in a wall-bounded channel. To set up a simple and fundamental situation, the channel consists of a pair of walls with flat and rough surfaces. Although the local aspect ratio based on the characteristic scale of the roughness may violate the condition for the Reynolds lubrication equation, streamlines away from the rough wall may exhibit less variational profile (see Fig. 1). Therefore, in this study, a streamline (and the velocity on the streamline) is used to impose the boundary condition for a lubrication equation; by redefining the reference gap width as the mean height of the streamline away from the rough wall (H' in Fig. 1), a sufficiently small aspect ratio H'/L' is readily available, and the pressure between the flat wall and streamline is obtained by solving a streamline-based lubrication equation. Then, the wall-normal variations of the pressure distribution between the flat and rough walls is reconstructed by considering higher-order terms through an extended lubrication model [17]. This higher-order lubrication model was originally developed for recovering the wall-normal pressure distribution from the wall pressure at a non-negligible aspect ratio, and the model has been validated through various problems including the permeation through a membrane induced by lubrication pressure [18, 19, 20] and the lubrication in a channel bounded by slip walls [21].

Through the above procedure, the meaning of the pressure that obeys the conventional Reynolds lubrication equation and its relation with the wall-normal distribution of the pressure are revealed, and the effectiveness of the proposed approach of the streamline-based lubrication model in a system with roughness is discussed.

This paper is organised as follows. Section 2 shows the basic equations used in this study and Section 3 explains the modelling strategy for analysing lubrication pressures. After establishing a method for solving lubrication flow with a sinusoidal roughness of a single wavenumber by including the wall-normal pressure distribution in Section 4, Section 5 extends the method for a more generalised case of sinusoidal roughness comprising multiple wave components. In both sections, the results are validated through comparison with analytical models obtained by a perturbation method in the Stokes regime. Finally, Section 6 summarises the above results.

2 Governing equations

For an incompressible Newtonian fluid of constant density ρ and viscous coefficient μ, the governing equations are the equation of continuity and the Navier-Stokes equations:

$$\nabla \cdot \boldsymbol{u} = 0 \,, \tag{1}$$

$$\rho \left(\frac{\partial \boldsymbol{u}}{\partial t} + \boldsymbol{u} \cdot \nabla \boldsymbol{u} \right) = -\nabla p + \mu \nabla^2 \boldsymbol{u} \,, \tag{2}$$

where t is the time, and $\boldsymbol{u}$ and p are the fluid velocity and pressure, respectively. In the following, two dimensional flow is considered, and the x and y components of the velocity are denoted as u and v, respectively. Non-dimensional variables are introduced as follows: $x_* = x/L$, $y_* = y/H$, $t_* = tU/L$, $u_* = u/U$, $v_* = v/\alpha U$, $p_* = p/\alpha^{-2}\mu U L^{-1}$ and $\alpha = H/L$, where L, H and U are the reference longitudinal length, the reference channel height, and the reference velocity, respectively, as illustrated in Fig. 1. For v_*, the order of magnitude for v is determined as αU from the equation of continuity. The non-dimensional forms of Eqs. (1) and (2) are $\nabla_* \cdot \boldsymbol{u}_* = \partial u_*/\partial x_* + \partial v_*/\partial y_* = 0$ and

$$\alpha^2 \mathrm{Re} \left(\frac{\partial u_*}{\partial t_*} + \boldsymbol{u}_* \cdot \nabla_* u_* \right) = -\frac{\partial p_*}{\partial x_*} + \alpha^2 \frac{\partial^2 u_*}{\partial {x_*}^2} + \frac{\partial^2 u_*}{\partial {y_*}^2} \,, \tag{3a}$$

$$\alpha^4 \mathrm{Re} \left(\frac{\partial v_*}{\partial t_*} + \boldsymbol{u}_* \cdot \nabla_* v_* \right) = -\frac{\partial p_*}{\partial y_*} + \alpha^4 \frac{\partial^2 v_*}{\partial {x_*}^2} + \alpha^2 \frac{\partial^2 v_*}{\partial {y_*}^2} \,, \tag{3b}$$

respectively, where $\mathrm{Re} = \rho U L/\mu$ is the Reynolds number. Assuming $\alpha^2 \mathrm{Re} \ll 1$, the above equations are reduced to the steady Stokes equation:

$$\frac{\partial p_*}{\partial x_*} = \alpha^2 \frac{\partial^2 u_*}{\partial {x_*}^2} + \frac{\partial^2 u_*}{\partial {y_*}^2} \,, \tag{4a}$$

$$\frac{\partial p_*}{\partial y_*} = \alpha^2 \left(\alpha^2 \frac{\partial^2 v_*}{\partial {x_*}^2} + \frac{\partial^2 v_*}{\partial {y_*}^2} \right) \,. \tag{4b}$$

Further assuming $\alpha \ll 1$ and if only the $O[\alpha^0]$ terms are retained, we obtain the following set of the reduced Stokes equations in the dimensional form:

$$\frac{\partial p}{\partial x} = \mu \frac{\partial^2 u}{\partial y^2} \tag{5a}$$

$$\frac{\partial p}{\partial y} = 0 \,. \tag{5b}$$

From the above equations along with the continuity equation, the Reynolds lubrication equation is derived with the no-slip boundary conditions at the smooth (or no-roughness) walls.

Furthermore, a higher-order effect of lubrication in a low Reynolds number flow (Re $\ll$ 1) can be relatively easily considered. For channel geometry of small curvature and small gradient (hereafter referred to as a moderately-varying surface profile), by retaining the terms of $O[\alpha^2]$ in Eq. (3), the following set of equations are obtained [17, 21]:

$$\frac{\partial p}{\partial x} = \mu \frac{\partial^2 u}{\partial y^2} \tag{6a}$$

$$\frac{\partial p}{\partial y} = \mu \frac{\partial^2 v}{\partial y^2} \; . \tag{6b}$$

The solution of the equations are given for the cases of no-slip boundary conditions [17] and slip-wall conditions [21] as

$$p(x, y) = p_{\mathrm{w}}(x) + p_{\mathrm{adj}}(x, y) \; . \tag{7}$$

The wall pressure $p_{\mathrm{w}}(x)$ obeys the Reynolds lubrication equation (i.e., the same equation obtained from Eq. (5)), and the adjusting component $p_{\mathrm{adj}}(x, y)$ is given as the longitudinal variation of the Couette-Poiseuille velocity profile driven by p_{w} and the wall velocities [17, 21]. For the case of no-slip walls (i.e., imposing Dirichlet boundary condition for the velocity) of the surface-to-surface distance $h(x)$, p_{adj} is solved in the following form [17]:

$$p_{\mathrm{adj}} = -\mu \frac{\partial}{\partial x} \left[-\frac{y(h-y)}{2\mu} \frac{\mathrm{d}p_{\mathrm{w}}}{\mathrm{d}x} + \frac{U_{\mathrm{r}}}{h} y \right] \; , \tag{8}$$

where U_{r} is the longitudinal component of the relative wall velocity.

3 Modelling strategy with rough wall

The above treatment was developed for a smooth and moderately-varying surface profile, and it is not applicable for rough surface which is often characterised with high-wavenumber components in the surface profile.

For a flow above a rough wall, imposing the boundary condition on the rough walls may not be suitable for constructing the lubrication equation, as the roughness wave length is usually smaller than the gap width. However, there may be a situation where a streamline away from the rough wall is smooth enough and the curvature and gradient of the streamline are sufficiently small.

In this study, Dirichlet boundary conditions are imposed for the velocities on a steady streamline (instead of the velocities on the rough wall), and the Reynolds lubrication equation based on the streamline and the corresponding higher-order pressure model are developed.

The pressure obtained from the streamline-based Reynolds lubrication equation is represented as p_{s}. In the limit of zero mean height H' of the streamline (see Fig. 1), the local aspect ratio $\alpha' \,(= H'/L')$ can be assumed to be sufficiently small, and the pressure p_{s} reasonably satisfies the assumption for the Reynolds lubrication equation. In this limit, p_{s} is represented as p_{w}, which is the wall pressure. Then, the wall-normal distribution of the pressure in the region between the flat and rough walls is modelled with a higher-order component added to the wall pressure $p_{\mathrm{w}}(x)$, just like Eq.(7).

As a deterministic approach, the lubrication model for the present geometry is derived by the following procedure:

1. Find an approximate stream function for the entire domain by perturbation method, assuming that the roughness is represented as a sum of high-wavenumber components with small amplitudes added to the nominal (i.e. flat) surface.

2. In a region sufficiently away from the rough wall, the geometry of the streamline and the velocity on the streamline are determined as explicit form.

3. With the velocity on the streamline as the Dirichlet boundary condition, the pressure p_{s} in the region bounded by the streamline and the flat wall is determined.

4. Find the wall pressure $p_{\mathrm{w}} \,(= \lim_{H' \to 0} p_{\mathrm{s}})$ by virtually moving the streamline towards the flat wall.

5. Find p_{adj} by the same procedure as in [17] for obtaining Eq. (8).

In the following sections, roughness profiles represented with a single wavenumber (§ 4) and a sum of multiple wavenumbers (§ 5) are considered. Through comparison of the pressure field obtained by the present models with reference solution, we show that two-dimensional pressure fields can be described with wall-tangential and wall-normal variations for both types of profiles, and that the above procedure can further be extended to a channel bounded by non-parallel nominal surfaces in Appendix.

Throughout the paper, we consider a situation that there is no flow separation above the rough surface.

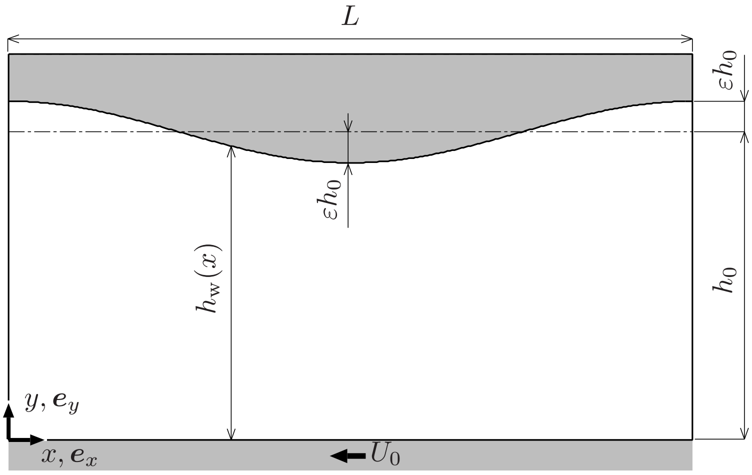

Figure 2: Schematic of a channel bounded by a flat wall and sinusoidal wall represented with a single wave superposed on a nominal (flat) surface in the upper side. The periodic boundary condition is applied in the x direction.

4 Case with a sinusoidal wall of a single wavenumber

4.1 Lubrication model

We consider a channel flow bounded by a stationary wavy wall of the following geometry:

$$h_{\rm w}(x) = h_0(\varepsilon \cos(kx) + 1) \tag{9}$$

and a flat wall moving at the velocity U_0, as schematically shown in Fig. 2. Here h_0 is the mean height of the wall, ε is the (non-dimensional) amplitude parameter, k is the wavenumber defined as $k = 2\pi/L$, and h_0 is the average height of the wavy wall. Periodic boundary condition is applied in the x direction, and the zero average pressure is assumed hereafter.

Assuming $\varepsilon \ll 1$, an approximate solution of the stream function is obtained from the perturbation method by following Refs. [22, 23]. Perturbation expansion of the stream function ψ is assumed to the following form:

$$\psi(x, y) \simeq \psi_0 + \varepsilon\psi_1 \ , \tag{10}$$

where ψ_0 is a stream function between two parallel (flat) plates with the distance h_0. With the boundary condition $\psi = 0$ on the top wall ($y = h_0$), ψ_0 takes the following form:

$$\frac{\psi_0}{h_0 U_0} = \frac{1}{2}\left(\frac{y}{h_0} - 1\right)^2 \ . \tag{11}$$

Substituting Eq.(10) into the Stokes equation (Eq.(4)), the bi-harmonic equation for ψ_1 is obtained [16]. The solution of ψ_1 takes the following form:

$$\frac{\psi_1}{h_0 U_0} = \left[\left(C_1 + C_2\frac{y}{h_0}\right)\sinh(ky) + \left(C_3 + C_4\frac{y}{h_0}\right)\cosh(ky)\right]\cos(kx) \ , \tag{12}$$

and the coefficients are obtained from the boundary conditions. From the no-slip boundary condition ($u = -U_0$, $v = 0$) on the lower wall ($y = 0$), we obtain

$$(C_1 k h_0 + C_4) \cos(kx) = 0 \,, \tag{13a}$$

$$C_3 k h_0 \sin(kx) = 0 \,. \tag{13b}$$

The no-slip boundary conditions on the upper wall are $\psi = 0$ and $\partial\psi/\partial n = 0$, where n is the coordinate in the wall-normal direction, and the following equations are obtained:

$$[(C_1 + C_2)\sinh(kh_0) + (C_3 + C_4)\cosh(kh_0)]\cos(kx) = 0 \,, \tag{14a}$$

$$\begin{aligned}&[(C_1 + C_2)kh_0 + C_4)\cosh(kh_0)\\ &+ (C_2 + (C_3 + C_4)kh_0)\sinh(kh_0) + 1]\cos(kx) = 0 \,.\end{aligned} \tag{14b}$$

From Eqs. (13) and (14), the coefficients in Eq. (12) are found as follows:

$$C_1 = \frac{\sinh(kh_0)}{\sinh^2(kh_0) - (kh_0)^2} \,, \tag{15a}$$

$$C_2 = \frac{kh_0\cosh(kh_0) - \sinh(kh_0)}{\sinh^2(kh_0) - (kh_0)^2} \,, \tag{15b}$$

$$C_3 = 0 \,, \tag{15c}$$

$$C_4 = -\frac{kh_0\sinh(kh_0)}{\sinh^2(kh_0) - (kh_0)^2} \,. \tag{15d}$$

The result uniquely determines the stream function Eq. (10) with Eq. (12), which coincides with Ref. [22] by the coordinate transformation z to $1 - y/h_0$. The streamline that goes through the point $(x, y) = (x_0, y_0)$ is identified as $\psi(x, y) = \psi(x_0, y_0)$. We select the point as $(kx, y/h_0) = (\pi/2, b)$ $(0 < b < 1)$ such that the perturbation term (ψ_1; Eq. (12)) becomes identically zero. The value of the stream function is as follows:

$$\hat{\psi} \overset{\text{def}}{=} \psi(\pi/2k, bh_0) = \frac{h_0 U_0}{2}(b - 1)^2 \,, \tag{16}$$

and the equation of the streamline that goes through the above point is expressed as

$$\psi(x, y) - \hat{\psi} = 0 \,. \tag{17}$$

To facilitate the subsequent treatments, we assume that Eq. (17) can be approximated as

$$y = h_{\mathrm{s}}(x) = h_0\,[\,a\cos(kx) + b\,] \qquad (0 < b < 1) \,, \tag{18}$$

which also goes through the same point. We further assume that the non-dimensional amplitudes a and ε to be sufficiently small such that the terms including a^2 or $a\varepsilon$ are negligible. By substituting Eq.(18) into Eq.(17), a is obtained (together with Eqs. (10) $\sim$ (12), (15) and (16)) as follows:

$$\begin{aligned} 0 &= \psi(x,y) - \hat{\psi} \\ &= (b-1)ah_0U_0\cos(kx) + \varepsilon h_0 U_0\big[(C_1+bC_2)\sinh(bh_0k) \\ &\quad + (C_3+bC_4)\cosh(bh_0k)\big]\cos(kx) + O(a^2, a\varepsilon, \varepsilon^2) \end{aligned} \tag{19}$$

$$\therefore \quad a = \varepsilon\frac{(C_1+C_2b)\sinh(bkh_0) + (C_3+C_4b)\cosh(bkh_0)}{1-b} \ , \tag{20}$$

which finally identifies the streamline in the form of Eq.(18) with b as the only parameter for the given geometry of roughness (i.e. fixed ε and k). As the streamline is eventually taken limit to the bottom wall ($b \to 0$), the Taylor expansion of a around $b = 0$ is taken as:

$$a \simeq \varepsilon k h_0 C_2^2 b^2 + O[b^3] \ ,$$

which guarantees the convergence of the streamline amplitude a to zero for $b \to 0$.

To prepare for the velocity boundary condition on the streamline, the longitudinal velocity at an arbitrary position is obtained:

$$u(x,y) = \frac{\partial\psi}{\partial y} = U_0\left(\frac{y}{h_0} - 1\right) + \varepsilon\frac{\partial\psi_1}{\partial y} \ . \tag{21}$$

By restricting y in the above equation to that of Eq. (18), and neglecting the terms that include a^2 or $a\varepsilon$, the velocity u_s on the streamline can be expressed as follows:

$$u_\mathrm{s} = U_0 c\cos(kx) + U_0 d \ , \tag{22a}$$

$$\begin{aligned} c = a + \varepsilon\,[&(C_1kh_0 + C_2bkh_0 + C_4)\cosh(bkh_0) \\ &+(C_2 + C_3kh_0 + C_4bkh_0)\sinh(bkh_0)] \ , \end{aligned} \tag{22b}$$

$$d = b - 1 \ . \tag{22c}$$

Finally, the pressure p_s in the region bounded by the streamline and the lower wall is determined using the geometry of the streamline (Eq.(18)) and the velocity on the streamline (Eq.(22a)) as Dirichlet boundary conditions. For a streamline far away from the rough wall, we can reasonably assume that p_s is independent of y and varies only with x. Integrating Eq. (6a) with respect to y, we obtain the following equation:

$$u = \frac{y^2}{2\mu}\frac{\mathrm{d}p_\mathrm{s}}{\mathrm{d}x} + U_0\left(C_5\frac{y}{h_0} + C_6\right) \ . \tag{23}$$

From the boundary conditions ($u = -U_0$ at $y = 0$ and $u = u_\mathrm{s}$ at $y = h_\mathrm{s}(x)$), the integration constants are found as follows:

$$C_5 = -\frac{h_\mathrm{s}}{2\mu}\frac{h_0}{U_0}\frac{\mathrm{d}p_\mathrm{s}}{\mathrm{d}x} + \frac{h_0}{h_\mathrm{s}}\left(\frac{u_\mathrm{s}}{U_0} + 1\right) , \tag{24a}$$

$$C_6 = -1 . \tag{24b}$$

From Eq. (23) and the continuity equation, we obtain

$$\frac{\partial v}{\partial y} = -\frac{\partial u}{\partial x} = -\frac{y^2}{2\mu}\frac{\mathrm{d}^2 p_\mathrm{s}}{\mathrm{d}x^2} - y\frac{U_0}{h_0}\frac{\mathrm{d}C_5}{\mathrm{d}x} , \tag{25}$$

and integrating with respect to y, we obtain the wall-normal component of the velocity as follows:

$$v = -\frac{y^3}{6\mu}\frac{\mathrm{d}^2 p_\mathrm{s}}{\mathrm{d}x^2} + U_0\left(-\frac{y^2}{2h_0}\frac{\mathrm{d}C_5}{\mathrm{d}x} + C_7\right) . \tag{26}$$

The boundary condition on the lower wall ($v = 0$ at $y = 0$) finds the integral constant C_7 to be zero. From the geometric condition, the velocity in the y direction on the streamline is imposed to be $v_\mathrm{s} = u_\mathrm{s}\mathrm{d}h_\mathrm{s}/\mathrm{d}x$. Then, the pressure equation is obtained as follows:

$$\frac{\mathrm{d}}{\mathrm{d}x}\left[\frac{h_\mathrm{s}^3}{12\mu}\frac{\mathrm{d}p_\mathrm{s}}{\mathrm{d}x}\right] = -\frac{U_0}{2}\frac{\mathrm{d}h_\mathrm{s}}{\mathrm{d}x} + \frac{\mathrm{d}}{\mathrm{d}x}\left[\frac{u_\mathrm{s}h_\mathrm{s}}{2}\right] . \tag{27}$$

This is the streamline-based Reynolds lubrication equation.

The pressure p_s is finally obtained as follows:

$$\frac{p_\mathrm{s}}{P_0} = \frac{6}{kh_0}\left[\frac{a(d-1)+2bc}{h_\mathrm{s}/h_0} - \frac{a(ac-bd+b)}{(h_\mathrm{s}/h_0)^2}\right]\frac{\sin(kx)}{a^2+2b^2} , \tag{28}$$

where $P_0 \stackrel{\mathrm{def}}{=} \mu U_0/h_0$ is the reference pressure, and the integration constants (when integrating Eq. (27) with respect to x) are determined such that the periodic boundary condition is satisfied in the x direction and the average pressure becomes zero.

Because a, c, and d are all determined by the mean height of the streamline bh_0 (see Eqs.(20), (22b), and (22c)), the pressure Eq.(28) is identified with the unique parameter b. Denoting the wavelength of the wavy wall as λ ($= L$ for the present case, Fig. 2), because the aspect ratio $\alpha' = bh_0/\lambda$ (for the region bounded by the streamline and the flat wall) is assumed to be small for the streamline-based Reynolds lubrication equation to be valid, the limit $b \to 0$ is taken for p_s, and the following form of the asymptotic boundary pressure $p_\mathrm{w}(x)$ is obtained:

$$\begin{aligned}\frac{p_\mathrm{w}(x)}{P_0} &= \lim_{b\to 0}\frac{p_\mathrm{s}(x)}{P_0} \\ &= 2\varepsilon kh_0\left[C_4 + 3\varepsilon C_2^2\cos(kx)\right]\sin(kx) .\end{aligned} \tag{29}$$

Note that this boundary pressure is constructed (in a form excluding the information of streamline geometry, but) only with the information of roughness geometry, which enables reconstruction of the two-dimensional pressure with a higher-order term (i.e. wall-normal component above the flat wall) as explained in the following.

Using the above asymptotic boundary pressure, the vertical distribution of pressure is reconstructed. From the higher-order lubrication model [17] for a relatively moderate geometry with small amplitude and curvature, the pressure distribution $p(x, y)$ in the entire domain is approximately given as

$$p_{\mathrm{M}}(x,y) = p_{\mathrm{w}}(x) + p_{\mathrm{adj}}(x,y) \ , \tag{30}$$

where p_{adj} is the adjustment to p_{w} in the order of magnitude as $O[p_{\mathrm{adj}}/p_{\mathrm{w}}] = \alpha'^2$ [17, 19], and the mathematical form of p_{adj} is given in the following. Integrating Eq. (6b) with respect to y yields the following equation:

$$\begin{aligned} p_{\mathrm{M}}(x,y) &= p_{\mathrm{w}}(x) + p_{\mathrm{adj}}(x,y) \\ &= \mu \frac{\partial v}{\partial y} \\ &= -\mu \frac{\partial u}{\partial x} \ . \end{aligned}$$

From Eqs. (23) and (29) and considering $\lim_{b \to 0} u_{\mathrm{s}}/h_{\mathrm{s}}$ (instead of U_{r}/h in Eq. (8)), the adjusting term p_{adj} is obtained as follows:

$$\begin{aligned} p_{\mathrm{adj}}(x,y) &= -\mu \frac{\partial}{\partial x} \left[\frac{y^2}{2\mu} \frac{\mathrm{d}p_{\mathrm{w}}}{\mathrm{d}x} + \mathit{\Gamma} y \right] \ , \\ \mathit{\Gamma} &= \frac{U_0}{h_0} \left[1 + 2\varepsilon k h_0 C_2 \cos(kx) \right] \ , \end{aligned} \tag{31}$$

and finally, the two-dimensional lubrication pressure with the rough wall is given as Eq.(30).

4.2 Discussion

To assess the validity of the proposed model, an analytical solution p_{A} is constructed with the stream function of Eq. (10) for the single-wavenumber roughness h_{w} (Eq.(9)). From the corresponding vorticity ω $(= -\nabla^2 \psi)$, pressure is obtained by solving the following equations:

$$\frac{\partial p_{\mathrm{A}}}{\partial x} = -\mu \frac{\partial \omega}{\partial y} \ , \tag{32a}$$

$$\frac{\partial p_{\mathrm{A}}}{\partial y} = +\mu \frac{\partial \omega}{\partial x} \ , \tag{32b}$$

and given as follows:

$$\frac{p_{\rm A}}{P_0} = 2\varepsilon k h_0 \left[C_2 \sinh(ky) + C_4 \cosh(ky)\right] \sin(kx) \ . \tag{33}$$

The distribution of $p_{\rm M}$ (Eq. (30)) and $p_{\rm A}$ (Eq. (33)) are compared in Figs. 3(a) and 3(b) at aspect ratio $\alpha = h_0/L = 0.1$ (equivalently $kh_0 = 2\pi\alpha$), wavy wall amplitude $\varepsilon = 0.1$, and Reynolds number $\mathrm{Re} = \rho UL/\mu = 0.01$. From the figures, the pressure distribution with the higher-order correction ($p_{\rm M}$) agrees well with $p_{\rm A}$. Figure 3(c) shows the pressure contours calculated by the method of Ref. [17] using Eqs. (7) with (8), where $p_{\rm w}$ is given as follows [17]:

$$p_{\rm w} = 6\mu U_0 \frac{2+\varepsilon\cos(kx)}{(h_0 k)^2\,(2+\varepsilon^2)} \frac{\varepsilon k \sin(kx)}{(1+\varepsilon\cos(kx))^2} \ . \tag{34}$$

As this method is suitable for a moderately-varying surface profile at aspect ratio $\alpha \lesssim 1$ and $\alpha^2 \ll 1$, the pressure distribution also shows reasonable agreement with $p_{\rm A}$.

By further increasing the aspect ratio to $\alpha = 0.5$ (with keeping the other parameters the same as the above case), the pressure distributions are compared in Fig. 3(d)–(f). This value of α is prohibitively large for the Reynolds lubrication model to be valid and a higher-order correction is necessary [17]. Although $p_{\rm M}$ (Fig. 3(d)) still reasonably reproduces the vertical distribution of $p_{\rm A}$ (Fig. 3(e)), the method of Ref. [17] underestimates the magnitude of the pressure as Fig. 3(f) shows. The difference between Fig. 3(d) and 3(f) suggests that the wall pressure, Eq. (29), obtained by solving the streamline-based lubrication equation provides better quality than Eq.(34) (obtained by the conventional Reynolds pressure equation applied to the region between wavy and flat walls) even at this value of aspect ratio α.

The average error in the modelled pressure p (two cases as explained later) from $p_{\rm A}$ is calculated at a fixed level $y = y_{\rm f}$ as follows,

$$E(p) \overset{\rm def}{=} \frac{1}{\lambda} \int_0^\lambda \left| \frac{p - p_{\rm A}}{p_{\rm A}} \right|_{y=y_{\rm f}} \mathrm{d}x \ , \tag{35}$$

where $\lambda = L$ in this section.

The following two cases are considered for p: (i) $p_{\rm s}|_{\psi=0}$ (i.e., solving the wall-based Reynolds lubrication equation with the wavy wall $\psi = 0$ as the boundary condition) and (ii) the present lubrication model $p_{\rm M}$ (i.e., using the streamline-based lubrication equation and reconstructing the vertical pressure distribution).

The average errors are shown in Fig. 4 as a function of aspect ratio α for two different $y_{\rm f}$ values, $y_{\rm f}/h_0 = 0.1$ and 0.8. Figure 4(a) plots $E\left(p_{\rm s}|_{\psi=0}\right)$, and the results indicates that the Reynolds lubrication equation is applicable only for a small α region, which coincides with the statement by Elrod [2]. When α becomes large, the assumptions for the Reynolds lubrication equation is violated and the errors in $p_{\rm s}|_{\psi=0}$

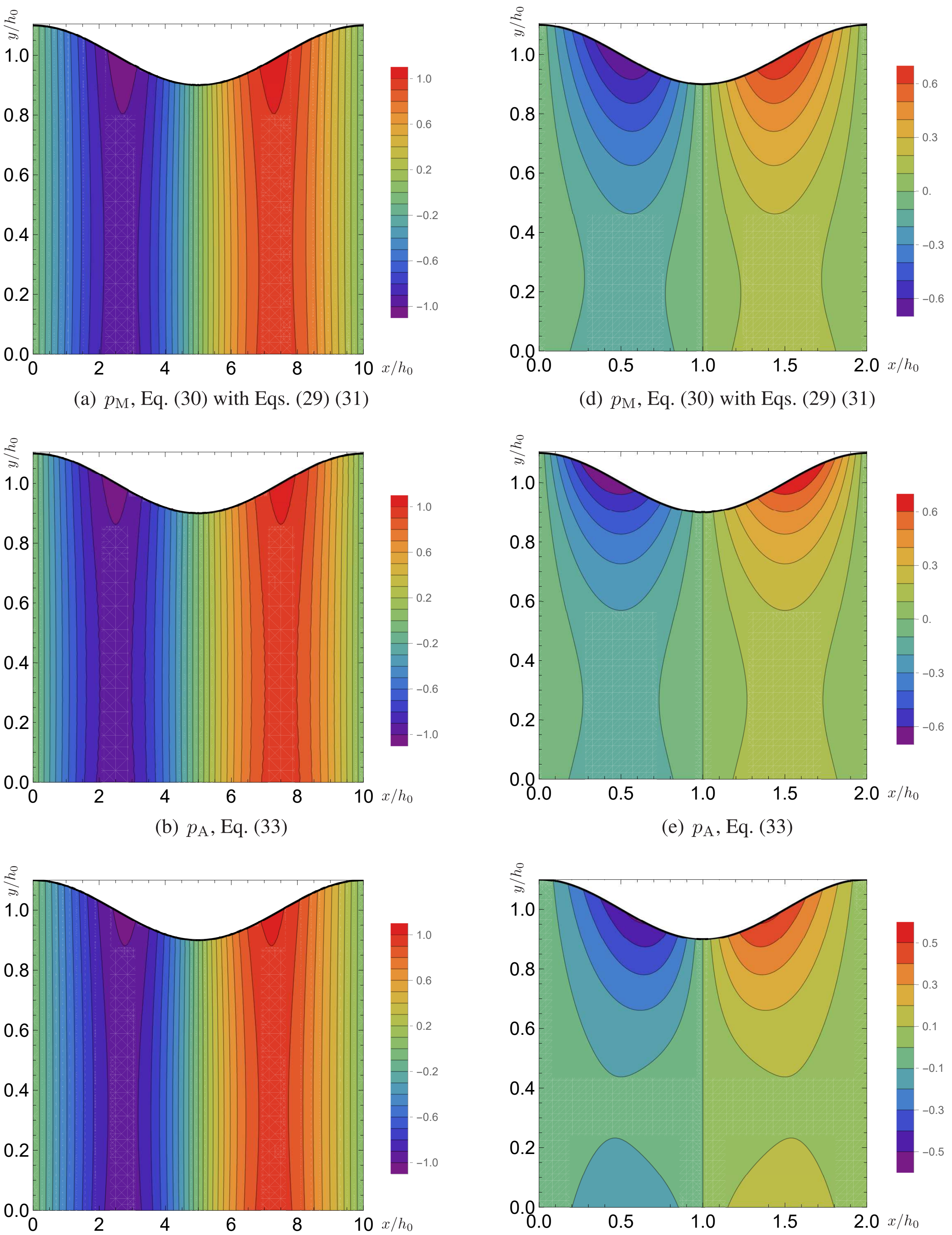

(a) p_{M}, Eq. (30) with Eqs. (29) (31)

(d) p_{M}, Eq. (30) with Eqs. (29) (31)

(b) p_{A}, Eq. (33)

(e) p_{A}, Eq. (33)

(c) Method by [17], Eq. (7) with Eqs. (8) (34)

(f) Method by [17], Eq. (7) with Eq.(8) (34)

Figure 3: Pressure contours in the channel bounded by flat and wavy walls with a single wavenumber of the wavenumber $kh_0 = 2\pi/10$ under the conditions of Reynolds number $\mathrm{Re} = 0.01$, the non-dimensional amplitude of the wavy wall $\varepsilon = 0.1$, and the aspect ratio (a)–(c) $\alpha = 0.1$ and (d)–(f) $\alpha = 0.5$. The pressures are obtained by (a)(d) the present lubrication model, (b)(e) solving Eq. (32), and (c)(f) the method in Ref. [17]. The pressure is shown normalised by $\mu U_0/h_0$.

are prohibitively large at both y_f levels. On the other hand, $E\,(p_\mathrm{M})$ in Fig. 4(b) shows that the mean errors are relatively small for both y_f levels. Although $E\,(p_\mathrm{M})$ shows local minima around $\alpha = 0.8$ or 0.9, this value of α is out of the applicable range of the higher-order lubrication model [17].

Figure 5 plots the error at $\alpha = 0.1$ as a function of the amplitude parameter of the wavy wall ε. The graph shows that the error develops almost linearly and a small value of ε guarantees a sufficiently small error level.

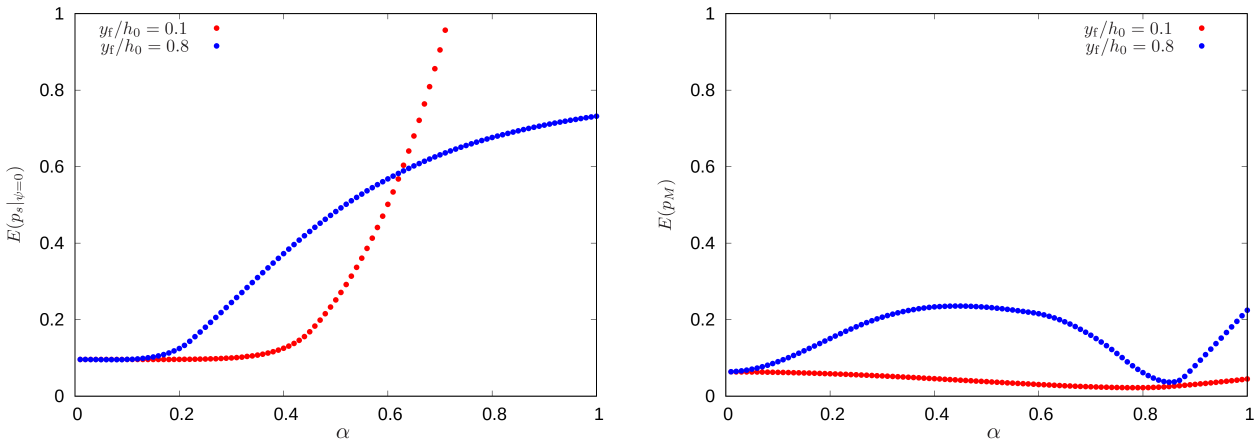

(a) Error in $p_\mathrm{s}|_{\psi=0}$ (b) Error in p_M

Figure 4: Average errors Eq.(35) in (a) $p_\mathrm{s}|_{\psi=0}$ and (b) p_M plotted as a function of the aspect ratio α under the Reynolds number $\mathrm{Re} = \rho U_0 L/\mu = 0.01$ and the non-dimensional amplitude of the wavy wall $\varepsilon = 0.1$.

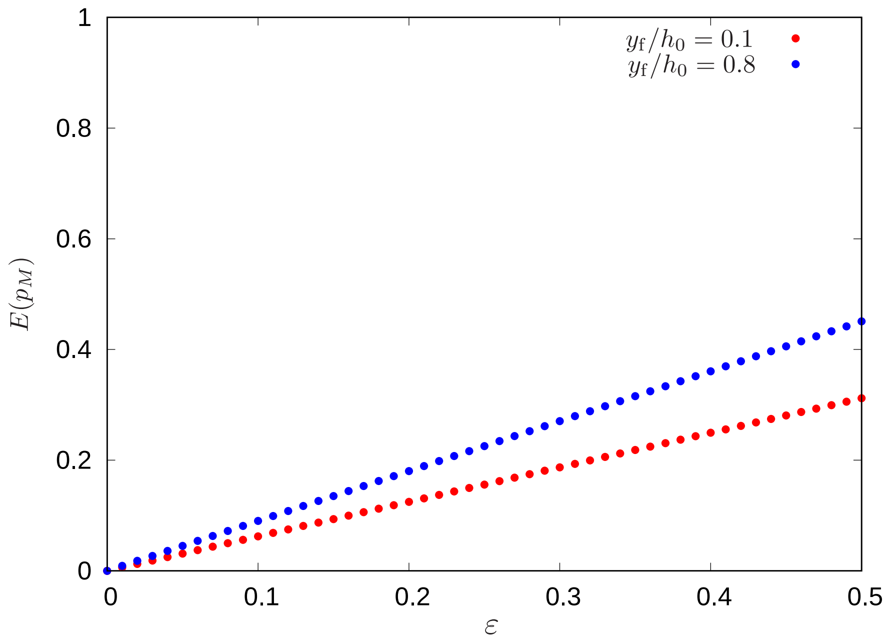

Figure 5: Average error in $E\,(p_\mathrm{M})$ against amplitude parameter of the wavy wall ε.

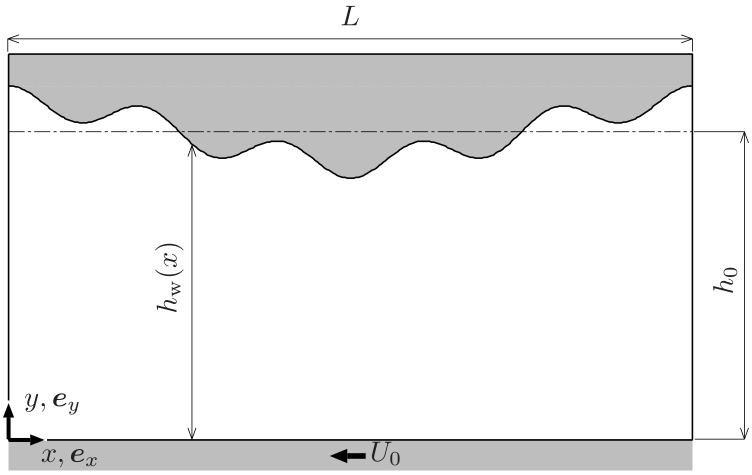

Figure 6: Schematic of a channel with a sinusoidal wall with a sum of multiple wave components (upper side) and a flat wall (lower side). The periodic boundary condition is applied in the x direction.

5 Case with multiple wavenumbers

The procedure in the previous section is extended to allow superposition of multiple waves as roughness, as schematically shown in Fig. 6. In this section, let the wavy wall shape be expressed by the following Fourier series:

$$h_\mathrm{w} = \varepsilon h_0 \sum_{i=1}^{n} \beta_i \cos(k_i x + \phi_i) + h_0 \ , \tag{36}$$

where h_0 is the mean height of the wall, and k_i and ϕ_i are the wavenumber and phase difference of the i-th wave component. To carry out a perturbation expansion, the amplitude parameter β_i is less than or equal to 1. The basic procedure is the same as in Section 4.

5.1 Lubrication model

Using the perturbation method to obtain the stream function, we obtain the following equations:

$$\psi \simeq \psi_0 + \varepsilon \psi_1 \ , \tag{37a}$$

$$\frac{\psi_0}{h_0 U_0} = \frac{1}{2}\left(\frac{y}{h_0} - 1\right)^2 \ , \tag{37b}$$

$$\frac{\psi_1}{h_0 U_0} = \sum_{i=1}^{n} \left[\left(C_{1i} + C_{2i}\frac{y}{h_0} \right) \sinh(k_i y) + \left(C_{3i} + C_{4i}\frac{y}{h_0} \right) \cosh(k_i y) \right] \cos(k_i x + \phi_i) \ , \tag{37c}$$

where

$$C_{1i} = \beta_i \frac{\sinh(k_i h_0)}{\sinh^2(k_i h_0) - (k_i h_0)^2} , \tag{38a}$$

$$C_{2i} = \beta_i \frac{k_i h_0 \cosh(k_i h_0) - \sinh(k_i h_0)}{\sinh^2(k_i h_0) - (k_i h_0)^2} , \tag{38b}$$

$$C_{3i} = 0 , \tag{38c}$$

$$C_{4i} = -\beta_i \frac{k_i h_0 \sinh(k_i h_0)}{\sinh^2(k_i h_0) - (k_i h_0)^2} . \tag{38d}$$

The geometry of the streamline h_s and the velocity u_s on the streamline are obtained in the following form:

$$h_\mathrm{s} = h_0 \sum_i a_i \cos(k_i x + \phi_i) + b h_0 \quad (0 < b < 1) , \tag{39a}$$

$$u_\mathrm{s} = U_0 \sum_i c_i \cos(k_i x + \phi_i) + U_0 d , \tag{39b}$$

Here, substituting Eq.(39) into the streamline equation (ψ) and assuming that the terms including $a_i a_j$ or $a_i \varepsilon$ ($1 \le i, j \le n$) are negligible, the coefficients a_i, c_i and d are obtained in the following functions of b:

$$a_i = \varepsilon \frac{(C_{1i} + C_{2i} b) \sinh(b k_i h_0) + (C_{3i} + C_{4i} b) \cosh(b k_i h_0)}{1 - b} , \tag{40a}$$

$$\begin{aligned} c_i = a_i + \varepsilon \, [&(C_{1i} k_i h_0 + C_{2i} b k_i h_0 + C_{4i}) \cosh(b k_i h_0) \\ &+ (C_{2i} + C_{3i} k_i h_0 + C_{4i} b k_i h_0) \sinh(b k_i h_0)] , \end{aligned} \tag{40b}$$

$$d = b - 1 . \tag{40c}$$

When solving the streamline-based pressure equation, the following approximations are applied for h_s^{-2} and h_s^{-3} for small a_i/b ($b \to 0$):

$$\frac{1}{h_\mathrm{s}^2} \simeq \frac{1}{b^2 h_0^2} \left(1 - 2 \sum_{i=1}^{n} \frac{a_i \cos(k_i x + \phi_i)}{b} \right) , \tag{41a}$$

$$\frac{1}{h_\mathrm{s}^3} \simeq \frac{1}{b^3 h_0^3} \left(1 - 3 \sum_{i=1}^{n} \frac{a_i \cos(k_i x + \phi_i)}{b} \right) , \tag{41b}$$

which are the differences from the procedure in Section 4 for integrating Eq. (27). Finally, by determining the integral constant to satisfy the periodic boundary conditions, the pressure p_s in the region between the flat wall and the streamline (Eq. (39a)) is obtained as follows:

$$\begin{aligned} \frac{p_\mathrm{s}}{P_0} = & \sum_{i=1}^{n} D_{5i} \sin(k_i x + \phi_i) + \sum_{i=1}^{n} D_{6i} \sin(2(k_i x + \phi_i)) \\ & + \sum_{i=1}^{n} \sum_{\substack{j=1 \\ (j \neq i)}}^{n} D_{7ij} \cos(k_i x + \phi_i) \sin(k_j x + \phi_j) , \end{aligned} \tag{42}$$

where

$$D_{5i} = \frac{6}{b^2 k_i h_0} \left(-\frac{3a_i}{b^2} \sum_{j=1}^{n} a_j c_j + \frac{-a_i + a_i d + bc_i}{b} \right) , \tag{43a}$$

$$D_{6i} = \frac{3a_i c_i}{b^3 k_i h_0} , \tag{43b}$$

$$D_{7ij} = \frac{12 k_j h_0 (a_j c_i + a_i c_j)}{b^3 \left(k_i^2 - k_j^2\right) h_0^2} . \tag{43c}$$

Taking the zero limit for the mean height of the streamline as $bh_0 \to 0$, the wall pressure $p_{\mathrm{w}}(= \lim_{b\to 0} p_s)$ is obtained as follows:

$$\frac{p_{\mathrm{w}}}{P_0} = \sum_{i=1}^{n} E_{5i} \sin(k_i x + \phi_i) + \sum_{i=1}^{n} E_{6i} \sin(2(k_i x + \phi_i)) + \sum_{i=1}^{n} \sum_{\substack{j=1 \\ (j \neq i)}}^{n} E_{7ij} \cos(k_i x + \phi_i) \sin(k_j x + \phi_j) \tag{44}$$

where $E_{mi} = \lim_{b\to 0} D_{mi}$ $(m = 5, 6)$ and $E_{7ij} = \lim_{b\to 0} D_{7ij}$, and these are given as follows:

$$E_{5i} = -\, 2\varepsilon (k_i h_0)^2 C_{1i} , \tag{45a}$$

$$E_{6i} = 6\varepsilon^2 k_i h_0 C_{2i}^2 , \tag{45b}$$

$$E_{7ij} = \frac{48\varepsilon^2 (k_i h_0)(k_j h_0)^2}{(k_i^2 - k_j^2) h_0^2} C_{2i} C_{2j} . \tag{45c}$$

The adjusting pressure term p_{adj} is obtained by the same equation as Eq. (31), and the coefficient Γ is given as follows:

$$\Gamma = \frac{U_0}{h_0} \left[1 + 2\varepsilon \sum_{i=1}^{n} k_i h_0 C_{2i} \cos(k_i x + \phi_i) \right] . \tag{46}$$

Finally, the pressure distribution is given as

$$p_{\mathrm{M}}(x, y) = p_{\mathrm{w}}(x) + p_{\mathrm{adj}}(x, y) . \tag{47}$$

Eq.(47) with Eqs. (31) and (44) is the general formula for the pressure distribution for a given geometry with multiple wavenumbers superposed on one side of a parallel-wall channel. More general extension of the above model to a rough wall in a non-parallel channel is presented in Appendix A.

5.2 Discussion

By solving Eq.(32), the analytical solution based on the perturbation expansion is obtained as follows:

$$\frac{p_{\mathrm{A}}}{P_0} = 2\varepsilon \sum_{i=1}^{n} k_i h_0 \left[C_{2i} \sinh(k_i y) + C_{4i} \cosh(k_i y) \right] \sin(k_i x + \phi_i) . \tag{48}$$

In this subsection, we set up a problem of superposing two wavenumbers: a surface of $k_1 h_0 = 2\pi/10$ (equivalent aspect ratio $\alpha_1 = k_1 h_0/2\pi = h_0/L = 0.1$) is added with the roughness of higher wavenumber $k_2 = 5k_1$. This wavenumber is chosen such that the corresponding wavelength $\lambda_2 = 2\pi/k_2 = L/5$ is sufficiently smaller than the longitudinal length scale L.

Figure 7 compares the pressure contour plots of (a) the lubrication model and (b) analytical solution obtained at Reynolds number $\mathrm{Re} = \rho U L/\mu = 0.01$ and the wavy wall amplitude parameters $\varepsilon = 0.1, \beta_1 = \beta_2 = 0.5$. The result shows that, although the wavelength λ_2 may be slightly out of the possible acceptable range (i.e., $\alpha_2 = h_0/\lambda_2 = 0.5$), the pressure distributions of p_M and p_A agree well for this two-wavenumber case.

The average relative error in p_M is defined as

$$E(p_\mathrm{M}) = \frac{1}{\lambda_\mathrm{max}} \int_0^{\lambda_\mathrm{max}} \left| \frac{p_\mathrm{M} - p_\mathrm{A}}{p_\mathrm{A}} \right| \mathrm{d}x \, , \tag{49}$$

where $\lambda_\mathrm{max} = \max\left[2\pi/k_1, 2\pi/k_2\right]$, and the error is plotted at two different heights $y_\mathrm{f}/h_0 = 0.1$ and 0.8 in Fig. 8 as function of α_2 with keeping the low wavenumber component k_1. Unlike the single-wavenumber case where the mean error increased with the aspect ratio (see Fig. 4(b)), the two-wavenumber cases exhibit an insensitive trend of the error against α_2. The major reason is that the reference pressure of the problem Eq. (4), $O\left[\mu U/\alpha_1^2 L\right]$, is much larger than the pressure induced by the wavenumber k_2, $O\left[\mu U/\alpha_2^2 L\right]$, and therefore, the relative errors remain at the similar level for different values of α_2, particularly in the higher region of α_2. This result indicates that the proposed method gives a reasonable pressure distribution for a roughness geometry given by a combination of small and large waves of wavelength sufficiently smaller than the channel scale L.

6 Conclusion

This study reveals a new aspect of lubrication pressure in a channel bounded by flat and rough surfaces to be described by a combination of wall pressure (obtained by streamline-based lubrication equation) and wall-normal pressure component obtained with the wall pressure.

By showing that the geometrical variation of the streamlines is sufficiently damped as the streamline goes away from the rough surface, a streamline-based lubrication equation is constructed with the velocity on the streamline as a boundary condition to establish the wall pressure on the flat wall. Then, the wall-normal variation of the pressure is recovered from the wall pressure and the wall velocity by a lubrication

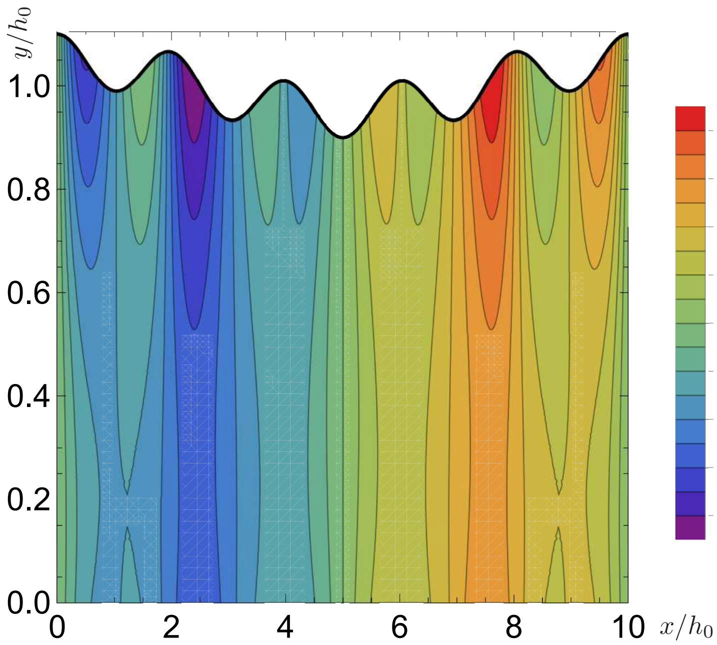

(a) p_{M}

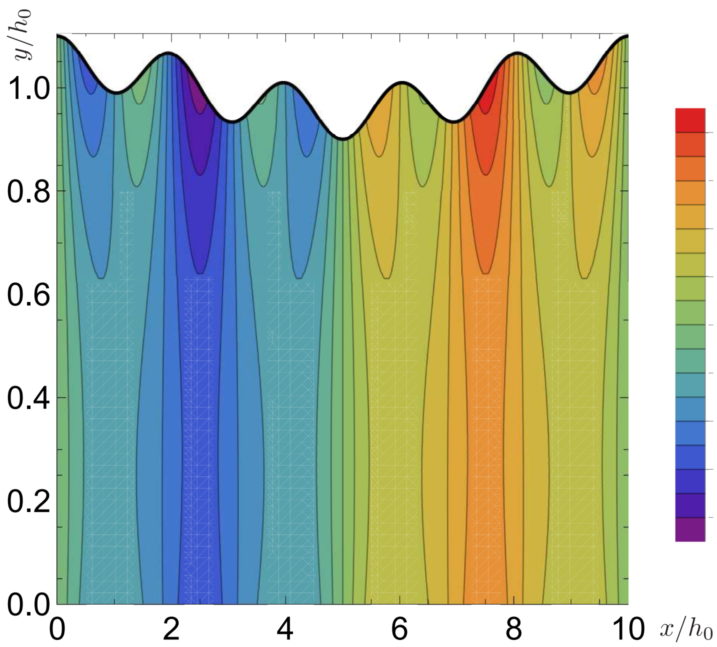

(b) p_{A}

Figure 7: Pressure contours in the channel bounded by flat and wavy walls with multiple wavenumbers obtained by (a) the present lubrication model and (b) solving Eq. (32), under the conditions of the wavenumbers $k_1 h_0 = 2\pi/10$ and $k_2 h_0 = \pi$, Reynolds number $\mathrm{Re} = 0.01$, and the non-dimensional amplitude of the wavy wall $\varepsilon = 0.1$. The pressure is shown normalised by $\mu U_0/h_0$.

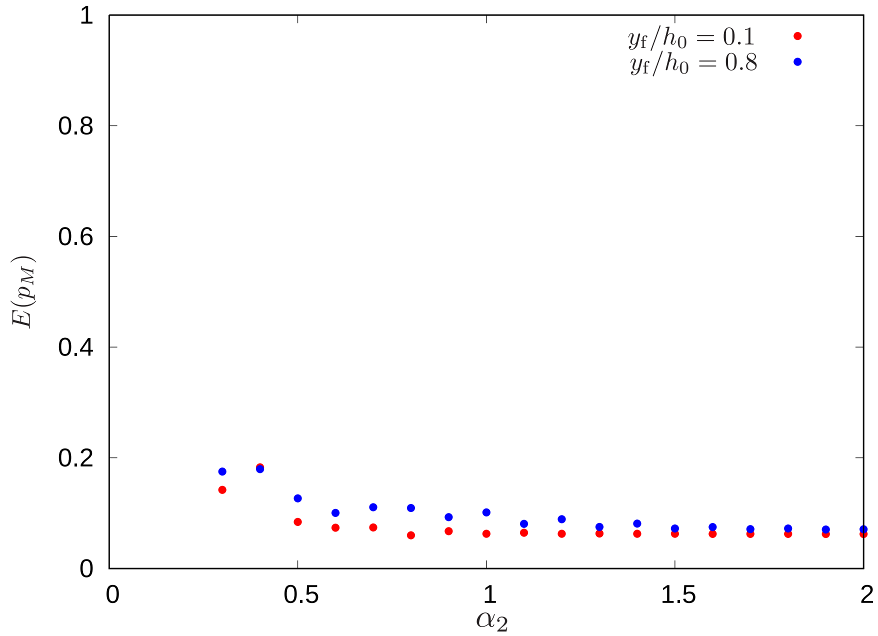

Figure 8: Average error Eq. (35) for p_M plotted as a function of the aspect ratio α_2 $(= k_2 h_0/2\pi)$ under the Reynolds number Re $= 0.01$ and the non-dimensional amplitude of the wavy wall $\varepsilon = 0.1$ and the amplitude parameter $\beta_1 = \beta_2 = 0.5$.

model that considers higher order terms. The applicable conditions of the proposed method are summarised as follows: (i) the roughness amplitudes are small and (ii) the higher wavenumbers in the roughness are sufficiently isolated from the lowest wavenumber (or the wavenumber of the nominal gap profile). The effectiveness of the proposed method is demonstrated through comparison with the pressure distribution obtained by a perturbation method for sinusoidal roughness of a single-wave component and two-wave components.

Although the second condition is not always practical for a case of superposed multiple sinusoidal components or general (random) roughness, the present study revealed the significance of the streamline-based lubrication equation (i.e. for the wall pressure) and the role of the higher-order term on the pressure variation in the wall-normal direction, which may provide effective view points to deeply understand the roughness lubrication and further develop a new approach for a case of non-parallel nominal surface as shown in Appendix.

Appendix

A Adding roughness to an arbitrary base shape $h_\mathrm{b}(x)$

In Sections 4 and 5, sinusoidal roughness is superposed on a flat wall of a parallel channel. In this section, sinusoidal roughness is superposed on a non-flat wall of weekly-undulating profile $h_\mathrm{b}(x)$ that satisfies

$|\mathrm{d}h_\mathrm{b}/\mathrm{d}x| \ll \min(\varepsilon\beta_i)\min(h_0k_i)/2\pi$, and the rough surface profile is given as follows:

$$h_\mathrm{w}(x) = \sum_{i=1}^{n} \varepsilon h_0 \beta_i \cos(k_i x + \phi_i) + h_\mathrm{b}(x)\ .$$

The stream function of form $\psi = \psi_0(x,y) + \varepsilon\psi_1$ is assumed, where ψ_0 is determined by the nominal geometry of the wall h_b. Following the same procedure as in Section 4, we find ψ_1 of the following form:

$$\psi_1 \simeq \sum_{i=1}^{n} \left[\left(C_{1i} + C_{2i}\frac{y}{h_0} \right) \sinh(k_i y) + \left(C_{3i} + C_{4i}\frac{y}{h_0} \right) \cosh(k_i y) \right] \cos(k_i x + \phi_i)\ . \tag{A1}$$

From the boundary conditions in Section 4, the coefficient are identified as follows:

$$C_{1i} = \beta_i \frac{h_\mathrm{b}}{h_0} \frac{\sinh(k_i h_\mathrm{b})}{\sinh^2(k_i h_\mathrm{b}) - k_i^2 h_\mathrm{b}^2} C_0\ , \tag{A2a}$$

$$C_{2i} = \beta_i \frac{k_i h_\mathrm{b} \cosh(k_i h_\mathrm{b}) - \sinh(k_i h_\mathrm{b})}{\sinh^2(k_i h_\mathrm{b}) - k_i^2 h_\mathrm{b}^2} C_0\ , \tag{A2b}$$

$$C_{3i} = 0\ , \tag{A2c}$$

$$C_{4i} = -\beta_i \frac{k_i h_\mathrm{b} \sinh(k_i h_\mathrm{b})}{\sinh^2(k_i h_\mathrm{b}) - k_i^2 h_\mathrm{b}^2} C_0\ , \tag{A2d}$$

where

$$C_0 = h_0^2 \left(\left.\frac{\partial^2\psi_0}{\partial y^2}\right|_{y=h_\mathrm{b}} - \frac{\mathrm{d}h_\mathrm{b}}{\mathrm{d}x} \left.\frac{\partial^2\psi_0}{\partial x \partial y}\right|_{y=h_\mathrm{b}} \right) \simeq h_0^2 \left.\frac{\partial^2\psi_0}{\partial y^2}\right|_{y=h_\mathrm{b}}\ . \tag{A3}$$

A streamline away from the roughness wall and the velocities on the streamline are used to impose boundary conditions for the lubrication pressure. Finding the streamline in a form of $h_\mathrm{s} = h_0 \sum a_i \cos(k_i x + \phi_i) + b h_\mathrm{b}$ and the velocity on the streamline as $u_\mathrm{s} = U_0 \sum c_i \cos(k_i x + \phi_i) + U_0 d$, the coefficients a_i, b, c_i, and d are obtained as follows:

$$\begin{aligned}
h_0 a_i =& -\varepsilon \frac{G_i^{1,2} \sinh(b k_i h_\mathrm{b}) + G_i^{3,4} \cosh(b k_i h_\mathrm{b})}{\partial\psi_0/\partial y|_{y=bh_\mathrm{b}}}\ ,\\
U_0 c_i =& a_i h_0 \left.\frac{\partial^2\psi_0}{\partial y^2}\right|_{y=bh_\mathrm{b}} + \frac{\varepsilon}{h_0}\left(k_i h_0 G_i^{1,2} + C_{4i}\right)\cosh(b k_i h_\mathrm{b})\\
&+ \frac{\varepsilon}{h_0}\left(k_i h_0 G_i^{3,4} + C_{2i}\right)\sinh(b k_i h_\mathrm{b})\ ,\\
U_0 d =& \left.\frac{\partial\psi_0}{\partial y}\right|_{y=bh_\mathrm{b}}\ ,
\end{aligned}$$

where

$$G_i^{1,2} = C_{1i} + \frac{b h_\mathrm{b} C_{2i}}{h_0}, \quad G_i^{3,4} = C_{3i} + \frac{b h_\mathrm{b} C_{4i}}{h_0}\ .$$

Assuming that the geometry of h_b is smooth and the Reynolds lubrication equation can be applied, the solution of the Reynolds lubrication equation with the boundary condition at $y = h_\mathrm{b}$ is denoted as p_s. With the corresponding higher order pressure p_adj, the pressure is given as $p = p_\mathrm{s} + p_\mathrm{adj}$. By taking the limit of $b \to 0$, p_adj under the roughness takes the following form:

$$p_\mathrm{adj} = -\mu \frac{\partial}{\partial x} \left[\frac{y^2}{2\mu} \frac{\mathrm{d}p_\mathrm{s}}{\mathrm{d}x} + \mathit{\Gamma} y \right] , \tag{A4}$$

where

$$\mathit{\Gamma}(x) = 2\varepsilon \sum_{i=1}^{n} k_i h_0 C_{2i} \cos(k_i x + \phi_i) + \left. \frac{\partial^2 \psi_0}{\partial y^2} \right|_{y=0} . \tag{A5}$$

Acknowledgements

This work is partly supported by Grants-in-Aid for Challenging Research (Exploratory) No. JP20K20972 and Grants-in-Aid for Scientific Research (B) No. JP23K01344 of the Japan Society for the Promotion of Science (JSPS).

Compliance with Ethical Standards

Conflict of interest: The authors declare that they have no conflict of interest.

References

[1] Reynolds, O., On the theory of lubrication and its application to Mr. Beuchamp towers experiments, including an experimental determination of the viscosity of olive oil. Philosophical Transactions of the Royal Society of London **177**, pp.157–234 (1886)

[2] Elrod, H.G., A review of theories for the fluid dynamic effects of roghness on laminar lubricating films, Technical Report No. 27, Columbia University, New York, (1977)

[3] Christensen, H., Stochastic models for hydrodynamic lubrication of rough surface, Proceedings of the Institution of Mechanical Engineers **184**, Issue 1, pp.1013–1026 (1969)

[4] Mitsuya, Y., A simulation method for hydrodynamic lubrication of surfaces with two-dimensional isotropic or anisotropic roughness using mixed average film thickness, Bulletin of JSME, **27**, Issue 231, pp.2036–2044 (1984)

[5] Patir, N. and Cheng, H.S., An average flow model for determining effects of three dimensional roughness on partial hydrodynamic lubrication, Journal of Lubrication Technology **100**, pp.12–17 (1978)

[6] Patir, N. and Cheng, H.S., Application of average flow model to lubrication between rough sliding surfaces, Journal of Lubrication Technology **101**, pp.220–230 (1979)

[7] Tripp, J.H., Surface roughness effects in hydrodynamic lubrication: the flow factor method, Journal of Lubrication **105**, pp.458–465 (1983)

[8] Sahlin, F., Almqvist, A., Larsson, R., Glavatskih, S., Rough surface flow factors in full film lubrication based on a homogenization technique, Tribology International **40**, pp. 1025–1034 (2007)

[9] Gu, J., Sakaue, M., Takeuchi, S., and Kajishima, T., An immersed lubrication model for the fluid flow in a narrow gap region, *Powder Technology* **329**, pp.445p-454 (2018)

[10] Hori, N., Rosti, M.E., Takagi, S. An Eulerian-based immersed boundary method for particle suspensions with implicit lubrication modelf, Computers and Fluids **236**, 105278 (2022)

[11] Asghar, Z., Elmoasry, A., Shatanawi, W., and Gondal M.A., An exact solution for directional cell movement over Jeffrey slime layer with surface roughness effects, Physics of Fluids **35**, 041901 (2023)

[12] Cabal, A., Szumbarski, J., Floryan, J.M., Numerical simulation of flows over corrugated walls, Computers & Fluids **30**, pp.753–776 (2001)

[13] Greenwood, J.A. and Williamson, J.B.P., Developments in the theory of surface roughness, 4th Leeds-Lyon Symp. Tribology, Roughness Effects in Lubrication, iv(i), pp. 167 (1977)

[14] Kovalchenko, A., Ajayi, O., Erdemir, A., Fenske, G., and Etsion, I., The effect of laser surface texturing on transitions in lubrication regimes during unidirectional sliding contact. Tribology International **38**(3), 21925 (2005)

[15] Jeong, J.-T. and Son, J., Stokes flow through a microchannel with periodical protuberances on the wall European Journal of Mechanics - B/Fluids **61**, Part 1, pp.9–15 (2017)

[16] Happel, J. and Brenner, H., *Low Reynolds Number Hydrodynamics*, Prentice-Hall (1965)

[17] Takeuchi, S. and Gu, J., Extended Reynolds lubrication model for incompressible Newtonian fluid, Physical Review Fluid **4**, No. 11, 114101 (2019)

[18] Takeuchi, S., Miyauchi, S., Yamada, S., Tazaki, A., Zhang, L. T., Onishi, R., and Kajishima, T. Effect of lubrication in the non-Reynolds regime due to the non-negligible gap on the fluid permeation through a membrane. Fluid Dynamics Research **53**, 035501 (2021)

[19] Takeuchi, S., Fukada, T., Yamada, S., Miyauchi, S., and Kajishima, T. Lubrication pressure model in a non-negligible gap for fluid permeation through a membrane with finite permeability. Physical Review Fluids Vol. **6**, No. 11, 114101 (2021)

[20] Yamada, S., Takeuchi, S., Miyauchi, S., and Kajishima, T. Transport of solute and solvent driven by lubrication pressure through non-deformable permeable membranes, Microfluidics and Nanofluidics **25**, 83 (2021)

[21] Takeuchi, S., Omori, T., Fujii, T., and Kajishima, T. Higher order lubrication model between slip walls, Microfluidics and Nanofluidics **27**, 46 (2023)

[22] Wang, C.-Y., Drag due to a striated boundary in slow Couette flow, Physics of Fluids **21**, No. 4, pp. 697–698 (1978)

[23] Pozrikidis, C. Creeping flow in two-dimensional channels, Journal of Fluid Mechanics **180**, pp. 495–514 (1987)

[24] Bayada, G. and Chambat, M., New models in the theory of hydrodynamic lubrication of rough surfaces, *ASME Journal Tribology* **110** pp. 402–407 (1988)

[25] Almqvist, A., Fabricius, J., Spencer, A., and Wall, P., Similarities and differences between the flow factor method by Patir and Cheng and homogenization, *ASME J. Tribology* **133**, 031702 (2011)